

Travelling to exotic places with cavity QED systems

Jonas Larson*

NORDITA, 106 91 Stockholm, Sweden

Recent theoretical schemes for utilizing cavity QED models as quantum simulators are reviewed. By considering a quadrature representation for the fields, it is shown how Jahn-Teller models, effective Abelian or non-Abelian gauge potentials, transverse Hall currents, and relativistic effects naturally arise in these systems. Some of the analytical predictions are verified numerically using realistic experimental parameters taking into account for system losses. Thereby demonstrating their feasibility with current experimental setups.

PACS numbers: 42.50.Pq, 71.70.Ej, 03.65.Vf, 73.43.-f

I. INTRODUCTION

Back in 2006 I was a co-author on a paper called “*Travelling to exotic places with ultracold atoms*” where we discussed some, at the time, new ideas how to mimic unusual phenomena occurring in condensed matter systems by using ultracold atoms [1]. Due to the controllability of system parameters and long decoherence times, cold atoms in optical lattices had shown to be suitable candidates for simulation of different many-body theories developed in the community of condensed matter physics [2]. Around the same time, many theoretical predictions were presented in which high energy and cosmological phenomena could be simulated by means of Bose-Einstein condensates [3]. In addition, ion-trap systems have recently drawn much attention in terms of simulating various spin chains as well as relativistic effects [4].

In the present proceeding I summarize some new directions employing cavity QED systems as quantum simulators. On the experimental side, cavity QED systems have seen great progress during the last years. Pure quantum effects are nowadays not restricted to single few-level atom-cavity setups [5], but include both quantum-dots (qdots) or SQUIDS [6] as well as Bose-Einstein condensates [7] coupled to single cavity modes. These new experiments pave the way for reaching the superstrong coupling regime where the strength of the effective matter-field coupling exceeds the system losses by several orders of magnitude. One crucial outcome of reaching this regime is that application of the rotating wave approximation (RWA) becomes questionable [8]. In most cases, going beyond the RWA implies that the corresponding system Hamiltonian is not integrable and other approximations or numerical methods are required. As outlined in Ref. [8], by expressing the cavity field(s) in its quadrature operators, it directly follows that beyond the RWA typical cavity QED models describe a set of coupled harmonic potentials. In this representation it is thereby possible to develop new physical intuition not easily extracted when the field is expressed in boson cre-

ation and annihilation operators. Moreover, in this picture the link between cavity QED models and systems from other fields of physics readily follows.

We consider a single N -level atom [9] coupled to a set of quantized cavity modes. The quadrature operators for mode k reads

$$\hat{X}_k = \frac{1}{\sqrt{2}} (\hat{a}_k + \hat{a}_k^\dagger), \quad \hat{P}_k = \frac{i}{\sqrt{2}} (\hat{a}_k - \hat{a}_k^\dagger) \quad (1)$$

with \hat{a}_k (\hat{a}_k^\dagger) the annihilation (creation) operator of a photon in mode k . The quadrature operators obey the canonical commutation relations $[\hat{X}_k, \hat{P}_l] = i\delta_{kl}$, and thereby can be viewed as “position” and “momentum” for the field. In the dipole approximation we assume the electric field $E(\mathbf{x})$ to be constant over the extent of the atom, hence letting $\mathbf{x} = \mathbf{0}$, to obtain

$$\bar{E} = \sum_k \bar{\varepsilon}_k \mathcal{E}_k \hat{P}_k, \quad (2)$$

where $\bar{\varepsilon}_k$ and \mathcal{E}_k are the polarization vector and the field amplitude of the k 'th mode respectively. Denoting the dipole moment between the atomic states $|i\rangle$ and $|j\rangle$ by \bar{d}_{ij} , the atom-field interaction takes the form

$$H_I = \sum_{i,j} \bar{d}_{ij} \cdot \bar{E}. \quad (3)$$

Due to selection rules or large atom-field detunings, most terms in the above sums vanish either exactly or approximately. Explicitly, the dipole moment $\bar{d}_{ij} = (d_{ij}^x, d_{ij}^y, d_{ij}^z)$, with $d_{ij}^\alpha = -e|i\rangle\langle i|\alpha|j\rangle\langle j| + \text{H.c}$ and e the electron charge. The full Hamiltonian, containing the free field and internal atomic energies, becomes

$$H = H_f + H_a + H_I, \quad (4)$$

where

$$H_f = \hbar \sum_k \omega_k \left(\frac{\hat{P}_k^2}{2} + \frac{\hat{X}_k^2}{2} \right), \quad H_a = \sum_{j=1}^N E_j |j\rangle\langle j|, \quad (5)$$

ω_k the frequency of mode k , and E_l being the energy of the j 'th initial atomic state.

*email: jolarson@kth.se

II. JAHN-TELLER SYSTEMS

Jahn-Teller systems frequently occur in both molecular/chemical physics and condensed matter physics [10]. The name dates back to the works by Hermann Jahn and Edward Teller studying symmetry breaking for polyatomic molecules [11]. Common for the Jahn-Teller models is that two potential surfaces become degenerate in a single point forming a *conical intersection*. About two decades after the pioneering work by Jahn and Teller, Longuet-Higgins showed that by encircling the degeneracy, the electronic wave function changes sign [12]. This phase factor was later realized to be the so called *Berry phase* [13].

A. The $\beta \times E$ model

The simplest non-trivial atom-cavity system considers a two-level atom interacting with a single cavity mode. Introducing the Pauli matrices $\hat{\sigma}_x = |1\rangle\langle 2| + |2\rangle\langle 1|$, $\hat{\sigma}_y = i(|1\rangle\langle 2| - |2\rangle\langle 1|)$, and $\hat{\sigma}_z = |1\rangle\langle 1| - |2\rangle\langle 2|$, the Hamiltonian reads

$$H_{\beta E} = \hbar\omega \left(\frac{\hat{P}^2}{2} + \frac{\hat{X}^2}{2} \right) + \frac{\hbar\Omega}{2} \hat{\sigma}_z + \hbar g \hat{\sigma}_x \hat{P}. \quad (6)$$

Here, Ω is the atomic transition frequency and g the effective atom-field coupling. Application of the RWA with respect to the first two terms renders the well known Jaynes-Cummings model [14]. For true atomic systems, it accurately explains several experimental observations [5]. In terminology of molecular physics, $H_{\beta E}$ is equivalent to the $\beta \times E$ Jahn-Teller Hamiltonian by simply interchanging \hat{X} and \hat{P} . For a deeper understanding of the dynamics, it is more convenient to think of $\hat{X}^2/2$ as the kinetic energy term and \hat{P} as the coordinate. In this picture, the *adiabatic potentials* are defined as

$$V_{ad}^{\pm}(\hat{P}) = \frac{\hbar\omega \hat{P}^2}{2} \pm \hbar\sqrt{\frac{\Omega^2}{4} + g^2 \hat{P}^2}. \quad (7)$$

The *diabatic potentials* are $V_d^{\pm}(\hat{P}) = \hbar\omega \hat{P}^2/2 \pm \hbar g \hat{P}$. Figure 1 depicts examples of the different potentials. Whenever $|g| > \sqrt{\omega\Omega}/2$, the lower adiabatic potential $V_{ad}^{-}(\hat{P})$ possesses two minima, while for $|g| < \sqrt{\omega\Omega}/2$ a single global minimum occurs at $P = 0$. The Jahn-Teller effect [10, 11] is easily understood from the adiabatic potentials; the amplitude of the ground state wave function does not attain its maximum at $P = 0$, but around the two shifted minima. For polyatomic molecules it implies that the conical intersection cause the molecule to vibrate around a less symmetric atomic configuration, or in other words, the ground state energy is decreased by lowering the symmetry. In terms of cavity QED, the Jahn-Teller effect states that for sufficiently strong atom-field coupling the ground state is not the one with the atom in its ground state and the field in vacuum. This effect has long

been known in cavity QED, and in the case of infinitely many atoms (the thermodynamical limit) it describes a second order quantum phase transition [15]. However, only recently has it been shown that this phase transition is identified as a Jahn-Teller symmetry breaking [16].

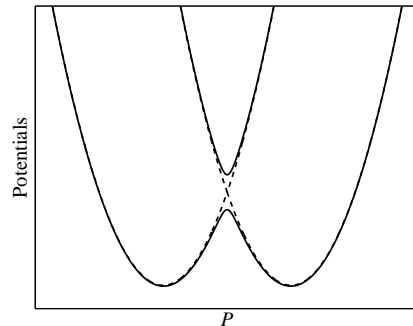


FIG. 1: Typical diabatic (dashed) and adiabatic (solid) potentials for the $\beta \times E$ model.

Before proceeding, some words of caution. The presence of a Jahn-Teller effect in the cavity QED setting is not possible by considering a direct coupling between the true atomic ground state and an excited state. A full microscopic derivation of the Hamiltonian contains a “self-energy” term that has been neglected. This is justified in most experimental situations, but in the $|g| > \sqrt{\omega\Omega}/2$ regime it can no longer be left out. Once this term is considered, sum-rules or gauge arguments can be employed to show that the lower adiabatic potential indeed never attains two minima [17]. In typical experiments, however, the atomic state $|g\rangle$ is not the true atomic ground state. Moreover, by utilizing Raman transitions the coupling is not direct and the above arguments do not apply. Longer discussions on this topic can be found in Refs. [16, 18].

B. The $\varepsilon \times E$ model

By considering a degenerate bimodal cavity, the $\beta \times E$ model can be extended to the $\varepsilon \times E$ one provided the atom-field couplings obey $\vec{d}_{eg} \cdot \vec{\varepsilon}_x \mathcal{E}_x = \hbar g \hat{\sigma}_x$ and $\vec{d}_{eg} \cdot \vec{\varepsilon}_y \mathcal{E}_y = \hbar g \hat{\sigma}_y$. We label the two modes by x and y . The Hamiltonian then takes the form

$$H_{\varepsilon E} = \hbar\omega \left(\frac{\hat{P}_x^2 + \hat{P}_y^2}{2} + \frac{\hat{X}^2 + \hat{Y}^2}{2} \right) + \frac{\hbar\Omega}{2} \hat{\sigma}_z + \hbar g \hat{P}_x \hat{\sigma}_x + g \hat{P}_y \hat{\sigma}_y, \quad (8)$$

with the adiabatic potential surfaces

$$V_{ad}^{\pm}(\hat{P}_x, \hat{P}_y) = \hbar\omega \frac{\hat{P}_x^2 + \hat{P}_y^2}{2} \pm \hbar\sqrt{\frac{\Omega^2}{4} + g^2 (\hat{P}_x^2 + \hat{P}_y^2)}. \quad (9)$$

Instead of having the double well structure as in Fig. 1, the lower adiabatic potential has a sombrero shape. This model was extensively studied in Ref. [16], focusing on

the effects due to the non-zero Berry phase acquired when encircling the conical intersection. Initializing a coherent state in one of the cavity modes such that it predominantly populate the lower adiabatic potential, it was demonstrated that over longer time periods population will be periodically swapped between the two modes and that this period greatly depends on the Berry phase.

C. Renner-Teller model

If the degeneracy is not conical it is glancing, meaning that the tangents of the two potential surfaces are identical. This defines the Renner-Teller models. The same type of Jahn-Teller effect is possible for Renner-Teller models, but the Berry phase vanishes whenever the intersection is in configuration space. From a physical point of view, the model we consider is thereby different since the intersection occurs in momentum space rather than in configurations space.

To achieve a glancing intersection we look at a three level Λ -atom with the two lower atomic states $|1\rangle$ and $|2\rangle$ coupled via two cavity modes to an excited state $|3\rangle$. The model Hamiltonian is taken as

$$H_{RT} = \hbar\omega \left(\frac{\hat{P}_x^2 + \hat{P}_y^2}{2} + \frac{\hat{X}^2 + \hat{Y}^2}{2} \right) + \sum_{j=1,2,3} E_j |j\rangle\langle j| + g \left(|3\rangle\langle 1| \hat{P}_x + |3\rangle\langle 2| \hat{P}_y + \text{H.c.} \right). \quad (10)$$

As a three-level system, there are three adiabatic and diabatic potential surfaces. Assuming degenerate modes and degenerate ground atomic states, $E_1 = E_2 = 0$, the adiabatic potentials become

$$V_{ad}^{\pm}(\hat{P}_x, \hat{P}_y) = \hbar\omega \frac{\hat{P}_x^2 + \hat{P}_y^2}{2} + \frac{E_3}{2} \pm \sqrt{\frac{E_3^2}{2} + g^2(\hat{P}_x^2 + \hat{P}_y^2)},$$

$$V_{ad}^0(\hat{P}_x, \hat{P}_y) = \hbar\omega \frac{\hat{P}_x^2 + \hat{P}_y^2}{2} \quad (11)$$

from which it is clear that $V_{ad}^-(\hat{P}_x, \hat{P}_y)$ and $V_{ad}^0(\hat{P}_x, \hat{P}_y)$ possess a glancing intersection at the origin.

III. EFFECTIVE GAUGE POTENTIALS

Gauge theories arise in a variety of fields in physics. For the most familiar case of a charged particle in an electromagnetic field the theory is Abelian. An example of a non-Abelian gauge theory is the one of Yang and Mills describing strong interaction. Getting an experimental handle of a system showing non-Abelian characteristics is therefore very attractive and has led to many suggestions. One possibility is adiabatically evolving systems either by means of external changes of the Hamiltonian or for ultracold atoms subjected to spatially varying light fields [19].

The general Hamiltonian (4) may be rewritten as

$$H = \hbar \sum_k \omega_k \left(\frac{(\hat{P}_k - \hat{A}_k)^2}{2} + \frac{\hat{X}_k^2}{2} \right) + \sum_j E_j |j\rangle\langle j| + \hat{\Phi}, \quad (12)$$

where

$$\hat{A}_k = -\sum_{i,j} \bar{d}_{ij} \cdot \bar{\epsilon}_k \mathcal{E}_k / \hbar\omega_k, \quad \hat{\Phi} = -\hbar \sum_k \omega_k \hat{A}_k^2. \quad (13)$$

The operators \hat{A}_k and $\hat{\Phi}$ have the properties as vector and scalar potential respectively. That is, they transform appropriately under unitary transformations [20]. For any atomic basis, these gauge potentials are matrices and they are said to be *Abelian* if $[\hat{A}_k, \hat{A}_l] = 0 \forall k$ and l and *non-Abelian* for non-commuting operators. As we now demonstrate, all three examples of the previous section render different types of gauge potentials.

A. Abelian gauge potential

As the atom-field interaction only includes a single mode for the $\beta \times E$ model, the vector potential consists of a single component which reads

$$A = -\frac{g}{\omega} \hat{\sigma}_x. \quad (14)$$

Consequently, the gauge potential is Abelian.

B. Non-Abelian $SU(2)$ gauge potential

For the second model, the $\varepsilon \times E$ one, we have

$$(\hat{A}_x, \hat{A}_y) = -\frac{g}{\omega} (\hat{\sigma}_x, \hat{\sigma}_y) \quad (15)$$

and hence $[\hat{A}_x, \hat{A}_y] = g^2 \hat{\sigma}_z / \omega^2$ showing that the gauge potential is non-Abelian.

Naturally, the dynamics is considerably richer for a system exhibiting non-Abelian structures. In general, time-ordering becomes important, *e.g.* enclosing a “loop” clockwise or anti-clockwise will not result in the same final system state. In Ref. [20], the time evolution of an initial state consisting of one empty mode and the other with a coherent state was numerically simulated. By properly choosing the phase of the coherent state, it will either set off clockwise or anti-clockwise around the conical intersection. Figure 2 displays an example of the atomic inversion $W(t) = \langle \hat{\sigma}_z \rangle$ during such time evolutions. The simulation utilizes realistic parameters of the qdot cavity QED experimented presented in [6], and furthermore takes into account for both cavity losses and atomic spontaneous emission. Solid and dotted lines corresponds to the different directions around the conical intersection of the coherent state. The difference between the two curves of the plot demonstrates the non-Abelian property.

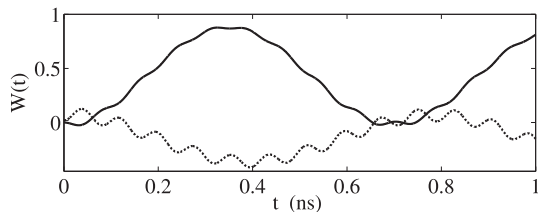


FIG. 2: Time evolved atomic inversion for an initial coherent state boosted clockwise (dotted) or anti-clockwise (solid) around the conical intersection of the $\varepsilon \times E$ model. Parameters can be found in Ref. [20].

C. Non-Abelian $SU(3)$ gauge potential

The last of our models, the Renner-Teller one, turns out to be non-Abelian as well. As a three-level system we express the gauge potential in Gell-Mann matrices

$$(\hat{A}_x, \hat{A}_y) = -\frac{g}{\omega}(\hat{\lambda}_4, \hat{\lambda}_6), \quad (16)$$

where $\hat{\lambda}_4 = |3\rangle\langle 1| + |1\rangle\langle 3|$ and $\hat{\lambda}_6 = |3\rangle\langle 2| + |2\rangle\langle 3|$. We note that $[\hat{A}_x, \hat{A}_y] = ig^2\hat{\lambda}_2/\omega^2$, with $\hat{\lambda}_2 = -i|1\rangle\langle 2| + i|2\rangle\langle 1|$.

IV. ANOMALOUS HALL EFFECT

In the condensed matter community, the coupling of our $\varepsilon \times E$ Hamiltonian is said to be on *Rashba spin-orbit* form [21]. It is known that such coupling gives rise to an effective Lorentz force inducing a transverse Hall current. The force is state dependent; opposite sign for the appropriate two internal states. When $\Omega = 0$, the population ratio between the two internal states is balanced and therefore the Rashba coupling brings about a transverse spin current [22]. A non-zero Ω breaks this symmetry and thereby it causes a net transverse particle current. Since the phenomenon derives from an intrinsic spin-orbit coupling, and not from an externally applied magnetic field as in the regular Hall effect, it has been termed *anomalous Hall effect* [23].

The net effective force acting on the state can be derived from

$$\bar{F} = \frac{d\dot{\bar{r}}}{dt} = \frac{1}{\hbar^2}[H, [H, \bar{r}]] = g(\bar{P} \times Z)\hat{\sigma}_z, \quad (17)$$

where $\bar{r} = (\hat{X}, \hat{Y})$, $\bar{P} = (\hat{P}_x, \hat{P}_y)$ is the momentum operators in the Heisenberg representation, and dot indicates time derivative. In quantum optics, the field is conveniently examined in phase space. The force (17) acts on the motion of the phase space distribution. Thereby, the Hall current occurs in phase space and hence does not involve a true particle current. In the quadrature representation it is clear that any field states evolving under the Hamiltonian (8) are bounded by a harmonic potential. Without the Rashba coupling a Gaussian coherent

state will bunch back and forth in the two-dimensional potential maintaining its shape. On the other hand, if the Rashba coupling is non-zero, the motion of the Gaussian wave packet will start to bend [24]. Hence, the rocking motion will be accompanied by a rotation around the Z -axis. This rotation is either clockwise or anti-clockwise depending on the internal atomic state. These assumptions are verified by propagating an initial state with mode x in a coherent state with amplitude $\alpha = 10/\sqrt{2}$, mode y in vacuum, and the atom in its lower state. The results are presented in Fig. 3 showing the trajectories of the averages $\langle \hat{X} \rangle$ and $\langle \hat{Y} \rangle$. It is seen that after hundreds of oscillations in the harmonic trap, all population has been transferred from the x to the y mode. The fact that the oscillating amplitude decreases during the evolution results from system losses.

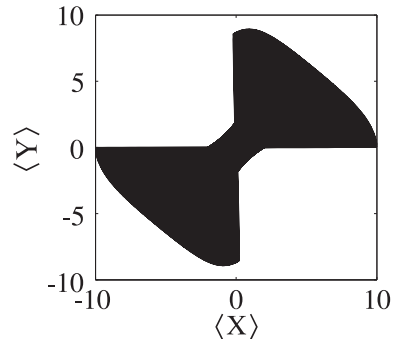


FIG. 3: Time evolution of the expectations $\langle \hat{X} \rangle$ and $\langle \hat{Y} \rangle$. Due to the transverse Hall current, the population initially residing in mode x is swapped to the y mode at the final time of propagation, which is after approximately 80 ns. The parameters are the same as those used in Fig. 2, and can be found in [24].

V. RELATIVISTIC EFFECTS

When conical intersections as the one of the $\varepsilon \times E$ model appears in momentum space they are frequently referred to as *Dirac cones*. Such Dirac cones have attracted a great amount of interests in especially the research of graphene. In the vicinity of the cones, the dispersions are linear as for free relativistic particles. The electrons of graphene may therefore show relativistic effects like for example *Zitterbewegung*. For avoided intersections the relativistic electrons have a non-zero effective mass, while for unavoided intersections the electrons are massless.

For small \hat{P}_x and \hat{P}_y we neglect the quadratic terms of the $\varepsilon \times E$ Hamiltonian

$$H_{rel} = \hbar g \sum_{k=x,y} \hat{\sigma}_k \hat{P}_k + \hbar \frac{\Omega}{2} \hat{\sigma}_z + V(\hat{X}, \hat{Y}). \quad (18)$$

This has the form of a Dirac equation for a spin-less particle moving within a two-dimensional harmonic potential

$V(\hat{X}, \hat{Y})$ [25]. The effective masses are equal but with opposite signs for the positive and negative energy solutions. In the present model, small values of \hat{P}_x and \hat{P}_y imply that the field amplitudes should be small, something easily achieved with ultracold high- Q cavities.

One interesting observation presented in [26] is that in the non-relativistic limit, the *Dirac oscillator* in 2+1 dimensions

$$H_{Do} = c\alpha \cdot (\mathbf{p} - im\beta\omega\mathbf{r}) + \beta mc^2, \quad (19)$$

with c the speed of light, \mathbf{p} and \mathbf{r} momentum and position respectively, $\alpha_k = \text{off} - \text{diag}(\hat{\sigma}_k, \hat{\sigma}_k)$, and $\beta = \text{diag}(1, -1)$, becomes identical to an $\varepsilon \times E$ Jahn-Teller Hamiltonian. Somewhat surprising is that the spin-less version of H_{Do} , in which the Dirac four-component matrices $\alpha_k \rightarrow \hat{\sigma}_k$ and $\beta \rightarrow \hat{\sigma}_z$, can be mapped onto the Jaynes-Cummings model [27]. Furthermore, even in the non-relativistic limit the trembling "motion" characterizing *Zitterbewegung* survives and is interpreted as the Ramsey interferometric effect [28].

VI. CONCLUSIONS

In this paper we have given a short summary how different cavity QED settings may serve as quantum simulators in various fields of physics. By working in a quadra-

ture representation for the fields, the dynamics of the combined atom-field system can be thought of as an artificial particle moving on a set of coupled potential surfaces. From thereon it is easy to identify different model Hamiltonians as Jahn-Teller ones. By rewriting these Hamiltonians, we defined effective gauge potentials, both Abelian and non-Abelian. Finally, we also demonstrated that relativistic effects should appear for weak field amplitudes.

From the list of references it is clear that it is only recently that these systems has been considered as quantum simulators. A natural conclusion thereby is that much more is to be discovered within this topic. To mention a few possibilities; spin Hall effects in for example the Renner-Teller model, Dicke models with multiple number of atoms, relativistic effects, spintronics.

This work did not cover a current proposal for simulation of Lipkin-Meshkov-Glick many-body model by means of cavity QED [29].

Acknowledgments

The author acknowledges support from the MEC program (FIS2005-04627) and Stig Stenholm for encouraging supervision during my PhD.

-
- [1] Lewenstein M, *et al.* 2006 *Atom. Phys.* **20** 869 201
 - [2] Lewenstein M *et al.* 2007 *Adv. Phys.* **56** 243
 - [3] Garay L *et al.* P 2000 *Phys. Rev. Lett.* **85** 4643
 - Stoof H T C *et al.* 2001 *Phys. Rev. Lett.* **87** 120407
 - [4] Johanning M *et al.* 2009 *J. Phys. B* **42** 154009
 - [5] Raimond J M & Haroche S 2006 *Exploring the Quantum* (Oxford: Oxford University Press)
 - [6] Schuster D I *et al.* 2007 *Nature* **445** 515
 - [7] Brennecke F *et al.* 2007 *Nature* **450** 268
 - Colombe Y *et al.* 2007 *Nature* **450** 272
 - [8] Larson J 2007 *Physica Scr.* **76** 146
 - [9] We will use the word "atom", but it is understood that it may also represent a qdot.
 - [10] Englman 1972 *The Jahn-Teller Effect in Molecules and Crystals* (New York: Wiley)
 - [11] Jahn H and Teller E 1937 *Proc. Roy. Soc. Lond. Ser. A* **161** 220
 - [12] Longuet-Higgins H C *et al.* 1958 *Proc. Roy. Soc. Lond. Ser. A* **244** 1
 - [13] Berry M V 1984 *Proc. Roy. Soc. Lond. Ser. A* **392** 45
 - [14] Jaynes E T & Cummings F W 1963 *Proc. IEEE* **51** 89
 - Shore B W & Knight P L 1993 *J. Mod. Opt.* **40** 1195
 - [15] Wang Y K & Hioe F T 1973 *Phys. Rev. A* **7** 831
 - [16] Larson J 2008 *Phys. Rev. A* **78** 033833
 - [17] Rzazewski K *et al.* 1975 *Phys. Rev. Lett.* **35** 432
 - Bialynicki-Birula & Rzazewski K 1975 *Phys. Rev. A* **19** 301
 - [18] Larson J & Lewenstein M 2009 *New J. Phys.* **11** 063027
 - [19] Wilczek & Zee A 1984 *Phys. Rev. Lett.* **52** 2111
 - Ruseckas J *et al.* 2005 *Phys. Rev. Lett.* **95** 010404
 - Larson J & Sjöqvist E 2009 *Phys. Rev. A* **79** 043627
 - [20] Larson J & Levin S 2009 *Phys. Rev. Lett.* **103** 013602
 - [21] Bychkov Y A & Rashba E I 1984 *J. Phys. C* **17** 6039
 - [22] Sinova J *et al.* 2004 *Phys. Rev. Lett.* **92** 126603
 - [23] Nagaosa *et al.* arXiv:0904.4154
 - [24] Larson J arXiv:0905.2829
 - [25] Thaller B 1992 *The Dirac Equation* (Berlin: Springer-Verlag)
 - [26] Moshinsky M & Szczepaniak A 1989 *J. Phys. A* **22** L817
 - [27] Bermudez A *et al.* 2007 *Phys. Rev. A* **76** 041801(R)
 - [28] Bermudez A *et al.* 2008 *Phys. Rev. A* **77** 033832
 - [29] Morrison S & Parkins A S 2008 *Phys. Rev. Lett.* **100** 040403
 - ibid.* 2008 *Phys. Rev. A* **77** 043810